J. Fluid Mech. (1974), *vol.* 63, *part* 4, *pp.* 635–640
Printed in Great Britain

The structure of jets of water and polymer solution in air

By J. W. HOYT, J. J. TAYLOR AND C. D. RUNGE
Naval Undersea Center, San Diego, California 92132

(Received 23 July 1973)

Jets of water and of poly(ethylene oxide) solutions discharging in air were photographed using a novel image-motion compensating camera. Spray droplet formation is inhibited by low concentration polymer solutions. The effect of the polymer is to reduce, dampen, or eliminate small-scale surface disturbances in the jet, while not reducing but even amplifying larger scale motions. The initial laminar zone present in the jet efflux with water is eliminated with trace quantities of polymer. When substantial quantities of polymer are present (200 p.p.m.), the jet breakup is accompanied by filament formation linking all the drops together.

1. Introduction

Striking changes occur in the visual appearance of a jet of water discharging into air when small amounts of a high polymer such as poly(ethylene oxide) are added to the flow. The rather ragged appearance of the water jet is transformed into a much more rod-like form as shown in the photograph (figure 1, plate 1), and this has attracted attention as a possible desirable attribute in fire-fighting (Green 1971). Yet the studies of Jackley (1966) and White (1967) using impact tube instrumentation, and Barker (1973) using a laser-Doppler velocimeter have all shown there is no discernable difference in gross structure (i.e. centre-line velocity, velocity profile, etc.) between water and polymer solution jets, in these cases, discharging under water. On the other hand, Hoyt (1971, 1972) found a large decrease in the cavitation inception parameter in jets discharged under water when polymers were present in the fluid.

Clearly the addition of polymers to these cases of turbulent fluid jet discharges causes a change in the flow, but this change has been apparently undetectable with the usual flow instrumentation. In order to shed more light on this problem, a special camera was developed for jet photography, and the jet appearance was recorded as a function of the nozzle size, polymer concentration and distance from the nozzle. The results show profound differences in the surface appearance of the jet as it is discharged from the nozzle, as it travels through the air and as it breaks up into spray when polymers are present in the flow.

Nominal	Actual average
10	6·7
50	39·6
200	177·8
2000	2202·5

TABLE 1. Polyox WSR-301 concentration (p.p.m.)

2. Technique

The principal experimental tool was an image-motion compensating camera, designed and developed as a private venture by one of the authors (JJT). In this camera, $2\frac{1}{4} \times 3\frac{1}{4}$ in. cut film is accelerated by high-speed rubber rollers (driven by a variable-speed motor) and passed behind the lens at a relatively constant velocity chosen to match the image speed to within a few per cent. The exposure is made by a short duration (15μs) electronic flash timed to occur when the film is in the centre of the lens. An alternative lighting arrangement is to use a narrow (0·02 in.) slit in the film plane, with relatively long duration lighting provided by flash bulbs. In each case, the jet was illuminated from behind, using a cloth diffuser in front of the flash source shaped to embrace 180° of the subject.

By moving the film at the same speed as the average motion of the image, exposures of *f*-16 to *f*-22 could be used with Eastman Kodak Plus-X and Tri-X film of ASA 320 (DIN 26) rating, thus ensuring good details in the negatives. All of the jet photos have been printed upside down so as to show the jet moving from left to right, which seems to aid visualization of the flow, although the actual camera set-up was in the opposite sense.

3. Experimental

Three nozzles were used in this study, with nominal jet diameters of $\frac{1}{8}$, $\frac{1}{4}$ and $\frac{1}{2}$ in. A straight run of 20 diameters of 2 in. pipe and a honeycomb flow straightener were installed ahead of the nozzle. The nozzles were supplied from a 500 gallon pressure tank which contained either water or a premixed polymer solution. A nozzle base pressure of 50 psi was used for all tests. Some of the water photos were made with water taken directly from the fire supply; no difference in appearance was noted. The jets were projected horizontally across the camera's field of view.

The polymer solutions were mixed in a separate tank and transferred to the pressure tank by gravity. Owing to uncertainties in estimating the quantities of water in the various tank elements, the polymer concentrations were set at a nominal value only. Samples were taken before and during each run, tested in the laboratory on the turbulent-flow rheometer (Hoyt 1965) and compared with a calibration curve for laboratory-mixed solutions from the same Polyox WSR-301 sample. Table 1 gives the average concentration compared with the nominal value.

Nozzle size	Location	Nominal polymer concentration (p.p.m.) 0	10	50	200	2000
$\frac{1}{8}$	In pipe	5·5	5	4·7	4	0·9
	Jet	87·5	79·5	74	64	14·6
$\frac{1}{4}$	In pipe	22	20	18·6	16	3·7
	Jet	175	159	148	128	29
$\frac{1}{2}$	In pipe	90	82	75	66	15
	Jet	350	318	297	255	58

TABLE 2. Estimated Reynolds numbers $\times 10^{-3}$

The estimated Reynolds numbers in the pipe feeding the nozzle and in the jet issuing from the nozzle were computed for each test case. These values, shown in table 2, were based upon viscosity measurements taken from Hoyt & Fabula (1964) for poly(ethylene oxide) of the same molecular weight.

Since it is known that poly(ethylene oxide) solutions have a lower air–liquid surface tension than water alone, a series of photos was taken with water in which the surface tension was reduced by the addition of the surfactant Aerosol 22. The resulting surface tension of the fluid was measured from samples using a duNouy surface tensiometer. No reduction in friction coefficient was noted from these samples when tested in the turbulent-flow rheometer.

The overall range of test parameters was thus three sizes of nozzle ($\frac{1}{8}$, $\frac{1}{4}$ and $\frac{1}{2}$ in. diameter) and five concentrations of polymer (0, 10, 50, 200 and 2000 p.p.m.) with photos taken at four locations (0, 3, 6 and 9 ft from the end of the nozzle).

4. Results

Photographs of jets as they emerge from the nozzle are given in figures 2–4 (plates 2–4) for the $\frac{1}{8}$, $\frac{1}{4}$ and $\frac{1}{2}$ in. diameter nozzles respectively. Turning first to the water jets (figures 2*a*, 3*a* and 4*a*), it appears that the jet structure is made up of an initially laminar region which then erupts into an unstable wave region as described by Landahl (1972). The initial laminar region occurs despite high initial Reynolds numbers (table 2) and can be attributed to the favourable pressure gradient in the nozzle. The lower initial Reynolds number and the larger contraction ratio in the $\frac{1}{8}$ in. diameter nozzle appear to result in a relatively longer zone of laminar flow than is seen for the larger nozzles.

Following transition, a series of eruptions occurs on the surface of the jet; Landahl (1972) attributes these to the springing forth of the curved ends of 'hairpin' vortices. The ends of these hairpin vortices then become spray droplets. Although there is considerable scatter in the results, the angles at which these spray vortices are seen in the photos are lower in the smaller nozzles than in the largest, the average angle being about 25° from the jet axis for the $\frac{1}{8}$ in. nozzle, 35° for the $\frac{1}{4}$ in. nozzle and 50° for the $\frac{1}{2}$ in. nozzle. This change, together with the marked increase in the number of spray vortices as the nozzle size increases, shows that the breakdown process is related to the momentum of the jet.

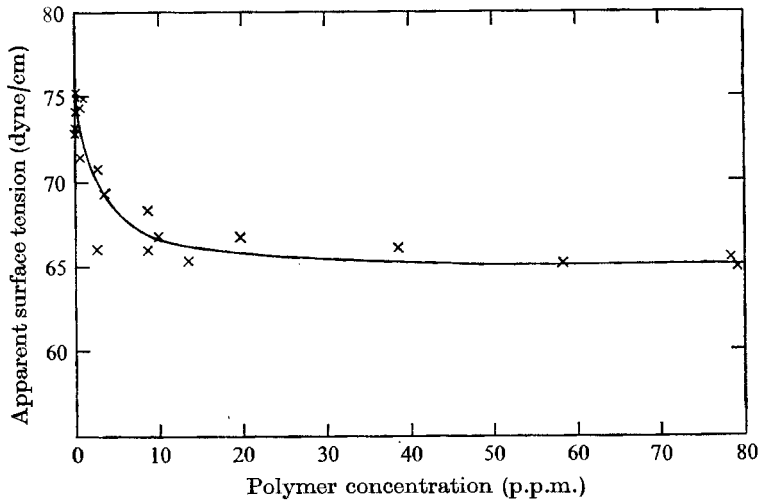

FIGURE 5. Measured air–liquid surface tension of poly(ethylene oxide) solutions.

Large changes occur in the surface of the jet when polymers are present in the fluid. As shown in figures 2(*b*), 3(*b*) and 4(*b*), with 10 p.p.m. poly(ethylene oxide) the initial laminar region does not appear. This could be related to the observations of Berman (1969) and Bilgen (1973), who noted that the velocity profile in entrance flows develops much faster for dilute polymer solutions than for water. In an inlet region, then, the polymer solution would have a shorter 'inlet length'.

Alternatively the effect could be considered as earlier transition to turbulence. In addition to this change, there is a substantial reduction in spray droplet formation.

As the polymer concentration is increased to 50 p.p.m. and above, spray formation ceases. If the spray formation is due to hairpin vortex eruption, it is evident that this type of boundary flow is greatly inhibited at all polymer concentrations studied. Since these polymer solutions have a greatly reduced friction in pipe flow compared with water, the reduction in spray formation may be analogous to the drag reduction mechanism, which seems to involve a reduction of turbulent bursts (Donohue, Tiederman & Reischman 1972).

At the highest polymer concentration, a laminar zone again appears as the jet leaves the nozzle. This is most pronounced with the $\frac{1}{8}$ in. diameter nozzle, which is the only one to show a laminar zone at 200 p.p.m. of polymer. The laminar zone may be due to the rather low entrance Reynolds number for the higher polymer concentrations or it may be a manifestation of viscoelasticity, for which the theory of Metzner & White (1965) predicts a greater inlet length. This is clearly brought out in the photographs. The wave structure on the surface of the jet appears most prominently in the photos of the highest concentration polymer.

Poly(ethylene oxide) solutions have a reduced air–liquid surface tension and figure 5 (from Hoyt 1971) shows how the surface tension varies with polymer concentration. In order to show that the jet effects are not related to this property of polymer solutions the $\frac{1}{8}$ in diameter nozzle was tested with surfactant solutions

having air–liquid surface tension of 50–38 dyne/cm. Figure 6 (plate 5) shows the resulting jet appearance and it seems evident that the changed surface tension plays only a small role in the major effects noted when polymers are present in the flow. The small effect of changed surface tension due to a surfactant was also noted by Dombrowski & Fraser (1954) in spray-nozzle photographic studies. They found that a freshly formed surface of surfactant solution may have the properties of the pure liquid, owing to the finite time required for the surfactant to act. The jet photographs were repeated with a 75 % solution of ethyl alcohol, having a surface tension of 26 dyne/cm. Figure 6 shows that surface-tension effects do not account for the observed polymer jet appearance.

Figures 7–9 (plates 6–8) and 10–12 (plates 9–11) show the appearance of jets from the $\frac{1}{4}$ in and $\frac{1}{2}$ in. nozzles at distances of 3, 6 and 9 ft from the nozzle exit respectively. Again it is clear that the addition of only trace quantities of polymer causes a major reduction in the spray droplets produced by the jet. These photos were taken with the camera in an image-motion, slot-exposure mode and it is important to remember that the photographs are a time history of the flow in a slice roughly 0·05 in. wide rather than a segment of the jet stopped in space. Ordinarily this causes no difficulty, but it would give an unusual effect close to the nozzle, for example.

The reduction in spray formation when polymers are present in the fluid is accompanied by an increase in the transparency and smoothness of the external surface of the jet stream. The effect of the polymer is thus to reduce, dampen or eliminate the small-scale surface disturbances while not reducing and in some cases even amplifying the larger scale motions.

The most striking changes in appearance come with the highest polymer concentration (200 p.p.m.), where jet breakup is accompanied by filament formation linking all drops together. The formation of filaments ('pituitousness') is a characteristic of compounds of high molecular weight in solution; its occurrence in the jet is evidence of high strain rates, presumably those produced by the large-scale instabilities of the jet.

The breakup of the jet appears to be related to the non-dimensional distance $S = X/d$, where X is the distance from the tip of the nozzle to the photograph location and d is the nozzle diameter. Figure 13 (plate 12) is a composite of photographs for several nozzle diameters and distances from the nozzle tip, in order to show how the breakup process is related to the non-dimensional distance S. It is evident that this is a controlling parameter in the breakup process.

By operating the camera in a two-lens two-slit mode, it was possible to obtain photographs of the same segment of the jet with a time interval displacement of approximately 0·0035 s. Figure 14 (plate 13) shows how the features of a polymer jet alter in this short time. The general axial movement appears to proceed regularly, but the displacements normal to the axis are rapid. The high strain rates thus induce 'thread-drawing' and pituitousness. Figure 15 (plate 14) shows a similar photograph for a disintegrating water jet.

These results confirm and extend the jet photographs of earlier workers. Goldin *et al.* (1969) noticed the initial nozzle behaviour and large amplitude wave formation before breakup of a turbulent 500 p.p.m. polyacrylamide jet. Hasegawa,

Tomita & Mochimaru (1972) show similar large amplitude wave formation in a turbulent jet of poly(ethylene oxide) solution. The technique used in this paper, however, allows much more detail to be discerned in the surface and structure of the jet. The large jets studied here also allow higher Reynolds numbers to be achieved, and these results may thus bear on the application of polymer jets in practical situations such as fire-fighting.

This work has been sponsored by the Fluid Dynamics Branch, Office of Naval Research, United States Navy.

REFERENCES

BARKER, S. J. 1973 Laser-Doppler measurements on a round turbulent jet in dilute polymer solutions. *J. Fluid Mech.* **60**, 721.

BERMAN, N. S. 1969 Flow behaviour of a dilute polymer solution in circular tubes at low Reynolds numbers. *A.I.Ch.E. J.* **15**, 137.

BILGEN, E. 1973 Behaviour of dilute polymer solutions in the inlet region of a pipe. *Trans. A.S.M.E. J. Appl. Mech.* E **40**, 381.

DOMBROWSKI, N. & FRASER, R. P. 1954 A photographic investigation into the disintegration of liquid sheets. *Phil. Trans.* A **247**, 101.

DONOHUE, G. L., TIEDERMAN, W. G. & REISCHMAN, M. M. 1972 Flow visualization of the near-wall region in a drag-reducing channel flow. *J. Fluid Mech.* **56**, 559.

GOLDIN, M., YERUSHALMI, J., PFEFFER, R. & SHINNAR, R. 1969 Breakup of a laminar capillary jet of a viscoelastic fluid. *J. Fluid Mech.* **38**, 689.

GREEN, J. H. 1971 Effect of polymer additives on nozzle stream coherence: a preliminary study. *Naval Undersea Centre Tech. Note*, no. 504.

HASEGAWA, T., TOMITA, T. & MOCHIMARU, Y. 1972 A study of anomalous turbulent flows of non-Newtonian fluids. *Bull. Japan Soc. Mech. Engrs*, **15**, 1093.

HOYT, J. W. 1965 A turbulent-flow rheometer. In *Symp. on Rheology* (ed. A. W. Marris & J. T. S. WANG). p. 71. New York: A.S.M.E.

HOYT, J. W. 1971 Effect of polymer additives on jet cavitation. *Proc. 16th Am. Towing Tank Conf.* Sao Paulo, Brazil.

HOYT, J. W. 1972 Jet cavitation in water containing polymer activities. *Proc. 13th Int. Towing Tank Conf.* Berlin.

HOYT, J. W. & FABULA, A. G. 1964 The effect of additives on fluid friction. *Proc. 5th Symp. Naval Hydrodyn.* p. 947. Bergen: Office of Naval Research, ACR-112.

JACKLEY, D. N. 1966 Drag reducing fluids in a free turbulent jet. *Naval Ordnance Test Station, NAVWEPS Rep.* no. 9053.

LANDAHL, M. P. 1972 Wave mechanics of breakdown. *J. Fluid Mech.* **56**, 775.

METZNER, A. B. & WHITE, J. W. 1965 Flow behaviour of viscoelastic fluids in the inlet region of a channel. *A.I.Ch.E. J.* **11**, 989.

WHITE, D. A. 1967 Velocity measurements in axisymmetric jets of dilute polymer solutions. *J. Fluid Mech.* **28**, 195.

(*a*)

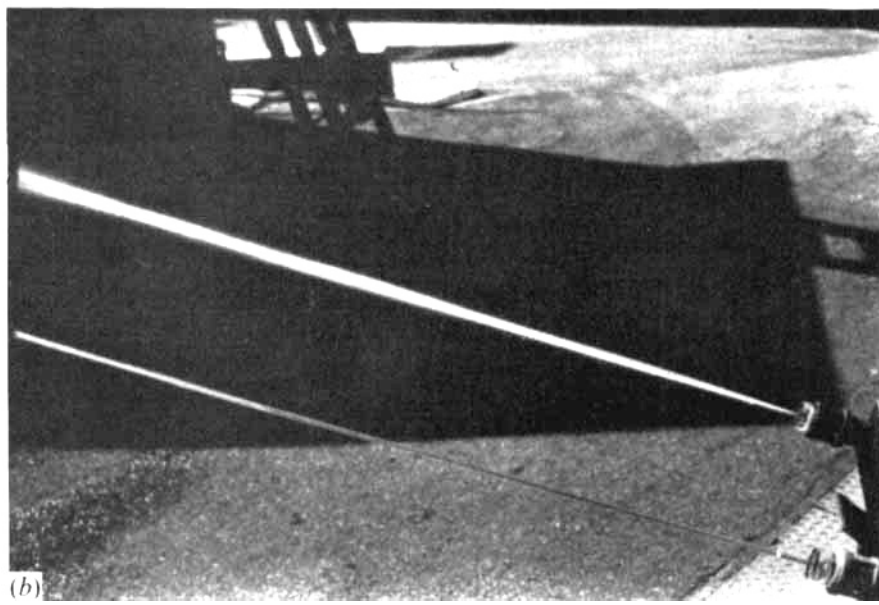

(*b*)

FIGURE 1. Evaluating 290 p.p.m. Polyox solution with $\frac{1}{4}$ in. nozzle. (*a*) Note spray from water stream on right. (*b*) Note rod-like polymer stream from lower nozzle.

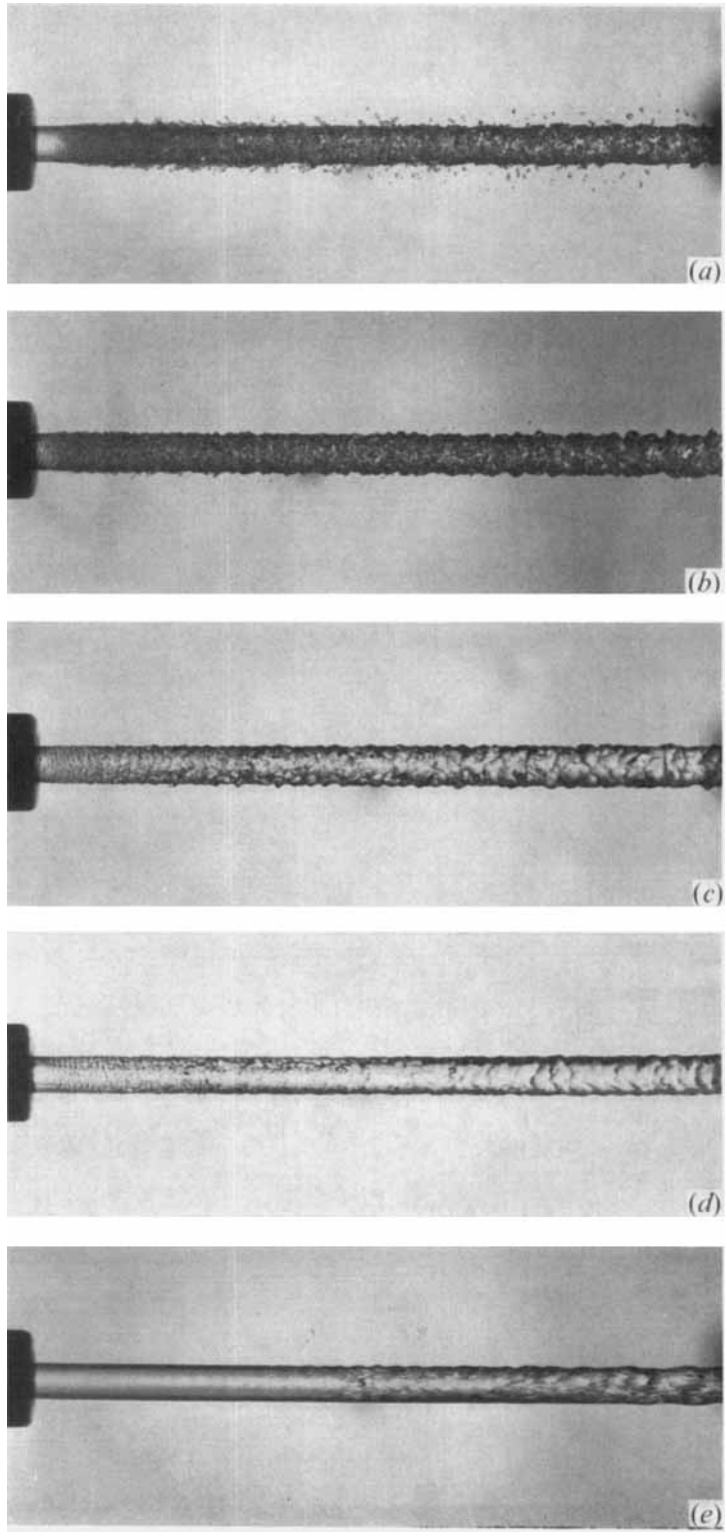

FIGURE 2. Flow at exit from $\frac{1}{8}$ in nozzle. (*a*) Water. (*b*) 10 p.p.m. poly(ethylene oxide). (*c*) 50 p.p.m. (*d*) 200 p.p.m. (*e*) 2000 p.p.m.

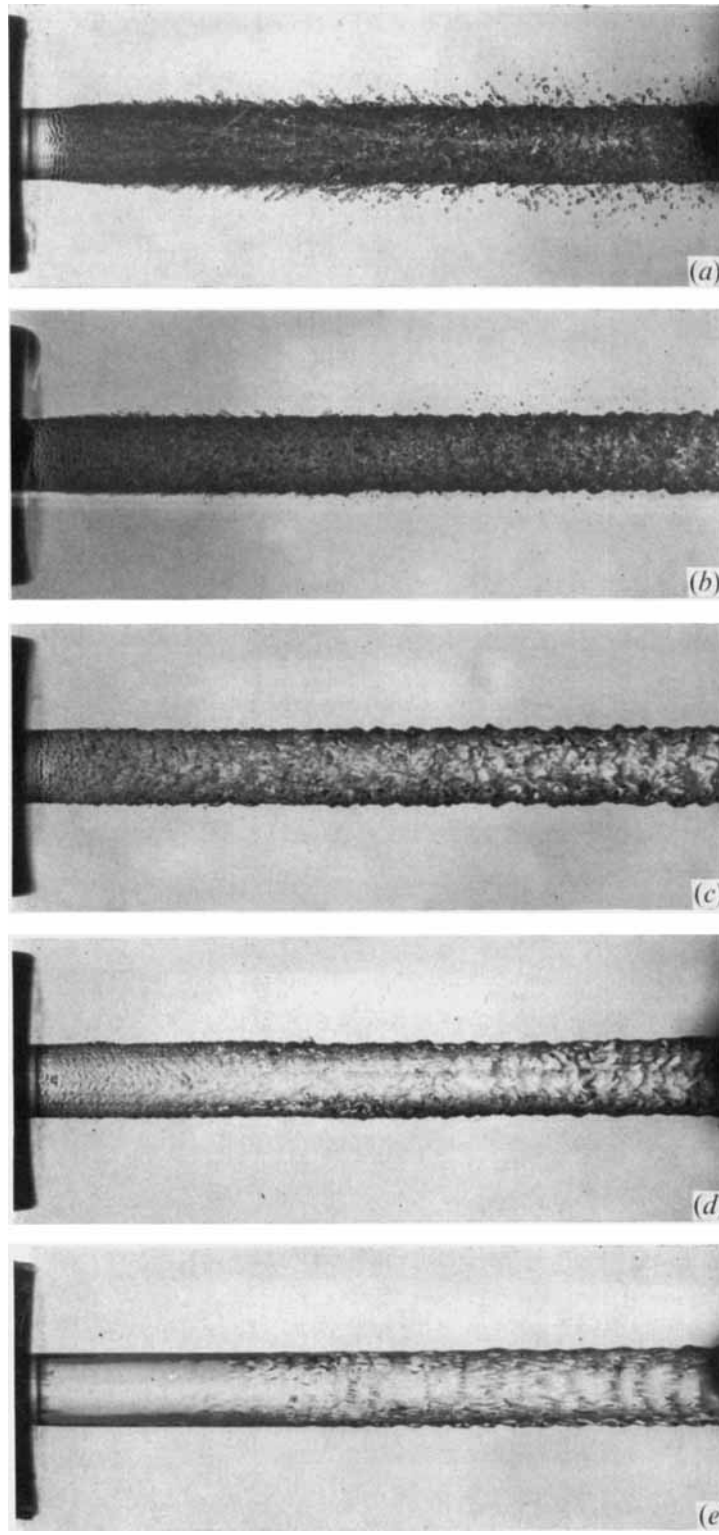

FIGURE 3. Flow at exit from $\frac{1}{4}$ in. nozzle. (*a*) Water. (*b*) 10 p.p.m. poly(ethylene oxide). (*c*) 50 p.p.m. (*d*) 200 p.p.m. (*e*) 2000 p.p.m.

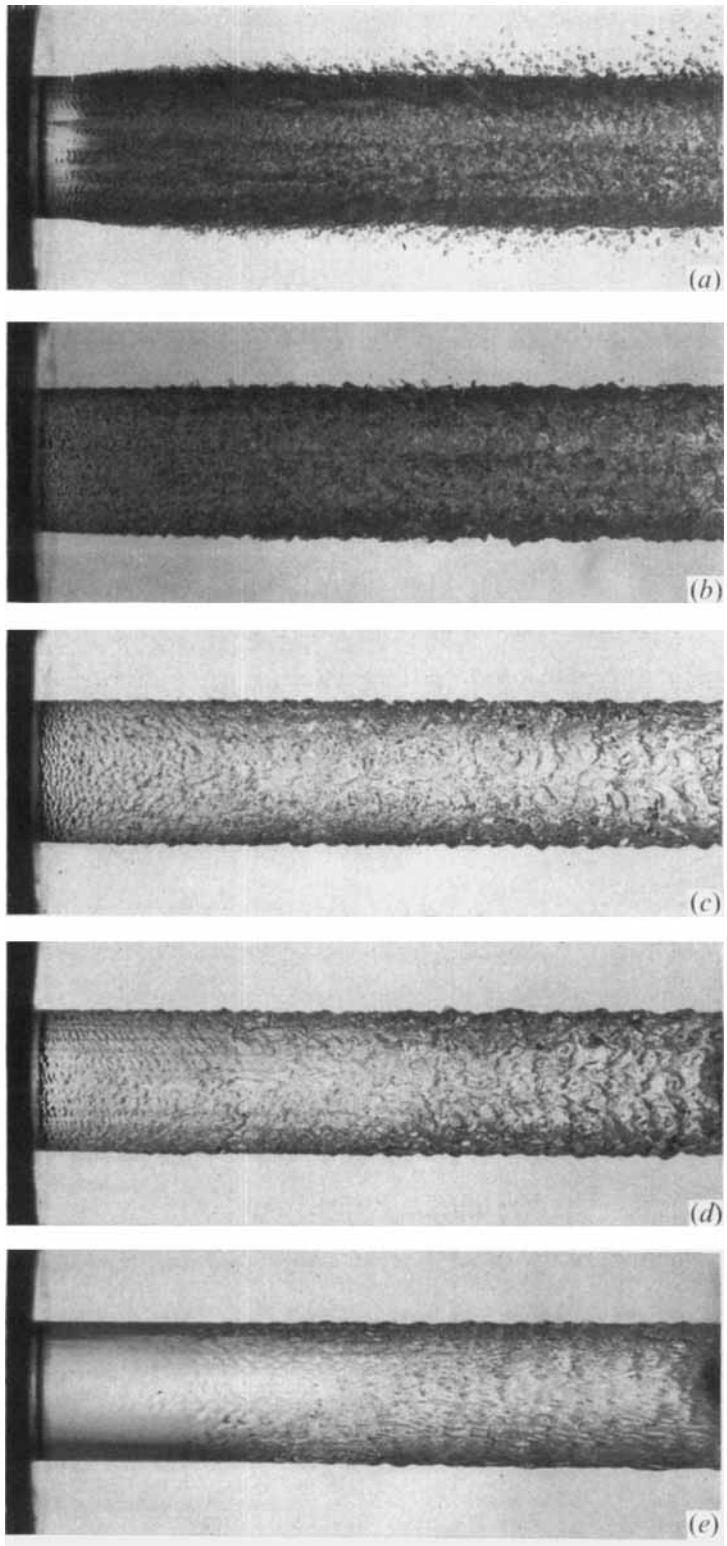

FIGURE 4. Flow at exit from $\frac{1}{2}$ in. nozzle. (*a*) Water. (*b*) 10 p.p.m. poly(ethylene oxide). (*c*) 50 p.p.m. (*d*) 200 p.p.m. (*e*) 2000 p.p.m.

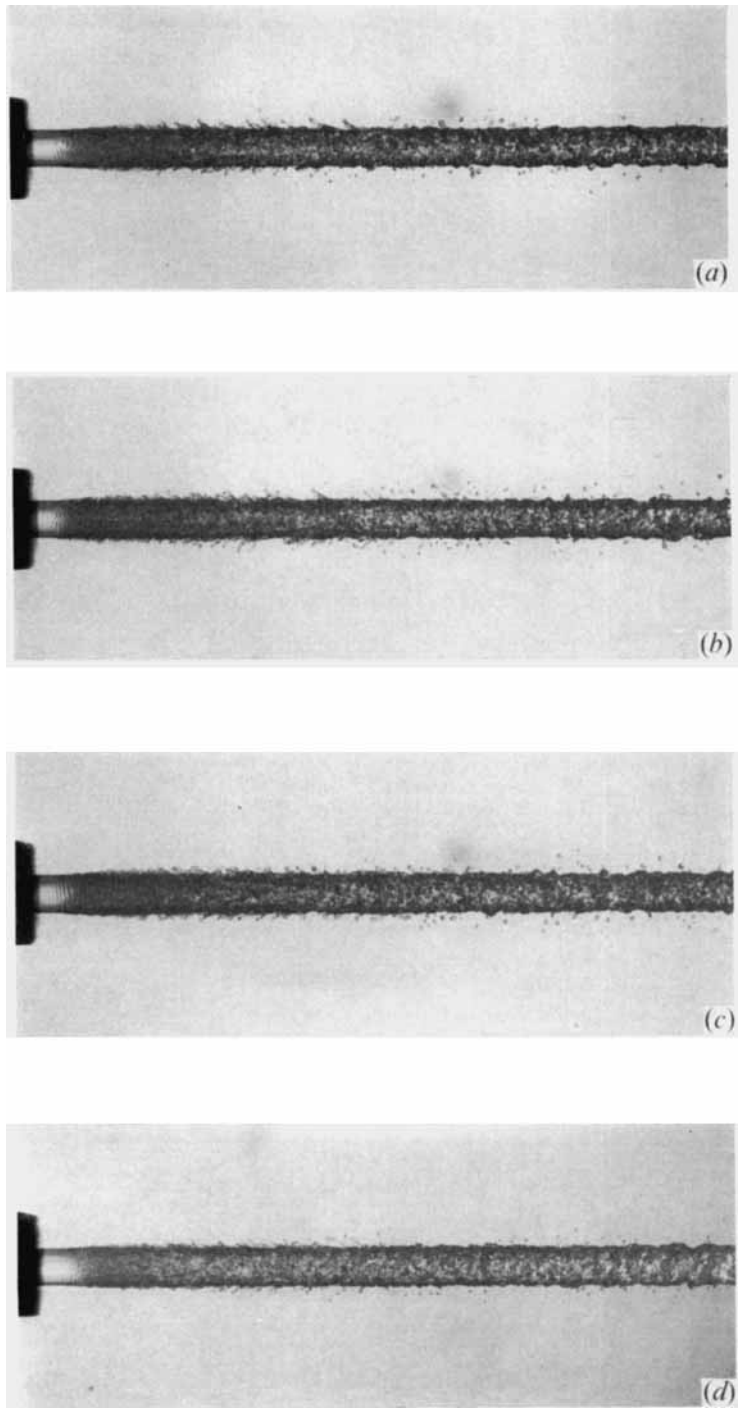

FIGURE 6. Appearance at exit of jet from $\frac{1}{8}$ in. nozzle. (*a*) Water. (*b*) Water with Aerosol 22, $\sigma = 50$ dyne/cm. (*c*) Water with Aerosol 22, $\sigma = 38$ dyne/cm. (*d*) Water–ethanol mixture, $\sigma = 26$ dyne/cm.

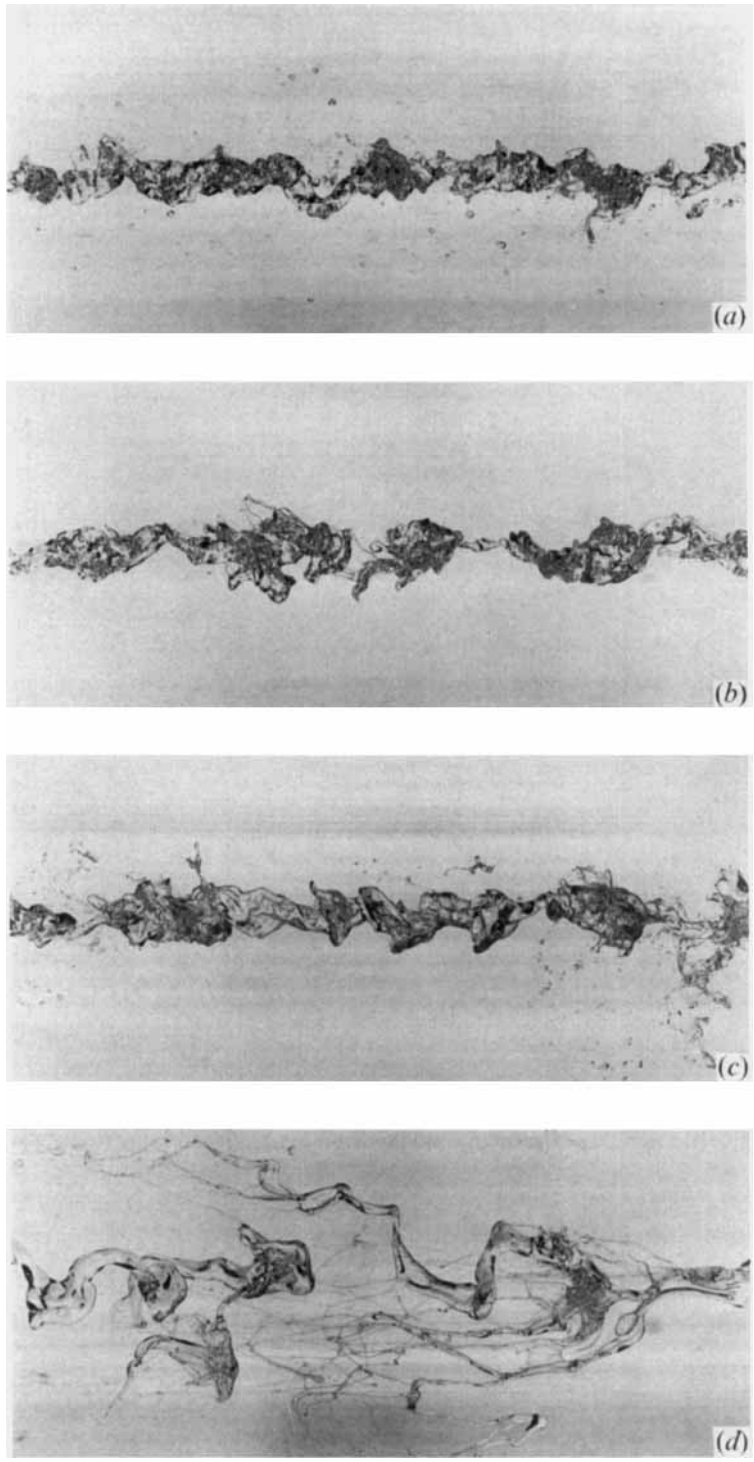

FIGURE 8. Appearance of jet from $\frac{1}{4}$ in. nozzle, 6 ft from nozzle exit. (*a*) Water. (*b*) 10 p.p.m. poly(ethylene oxide). (*c*) 50 p.p.m. (*d*) 200 p.p.m.

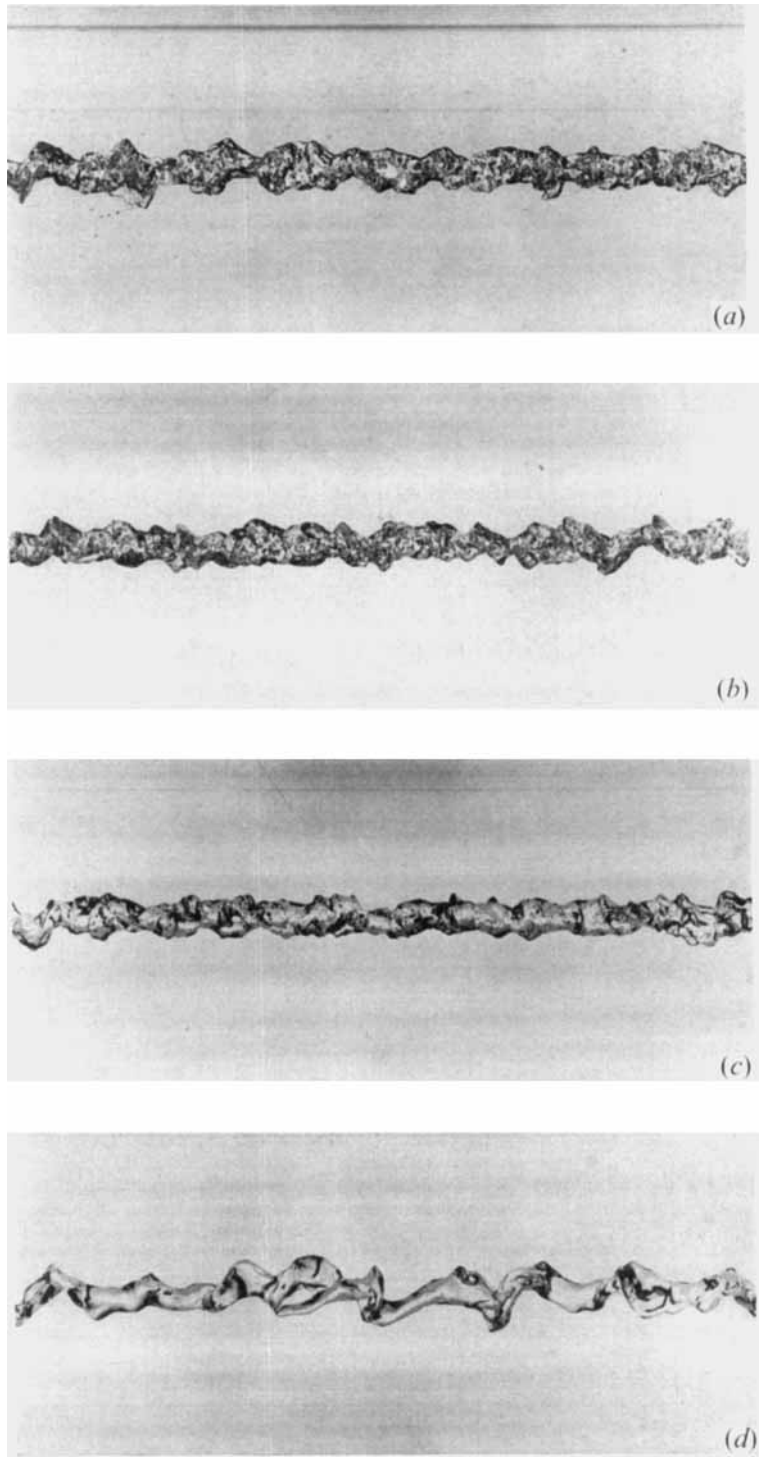

FIGURE 7. Appearance of jet from $\frac{1}{4}$ in. nozzle, 3 ft from nozzle exit. (*a*) Water. (*b*) 10 p.p.m. poly(ethylene oxide). (*c*) 50 p.p.m. (*d*) 200 p.p.m.

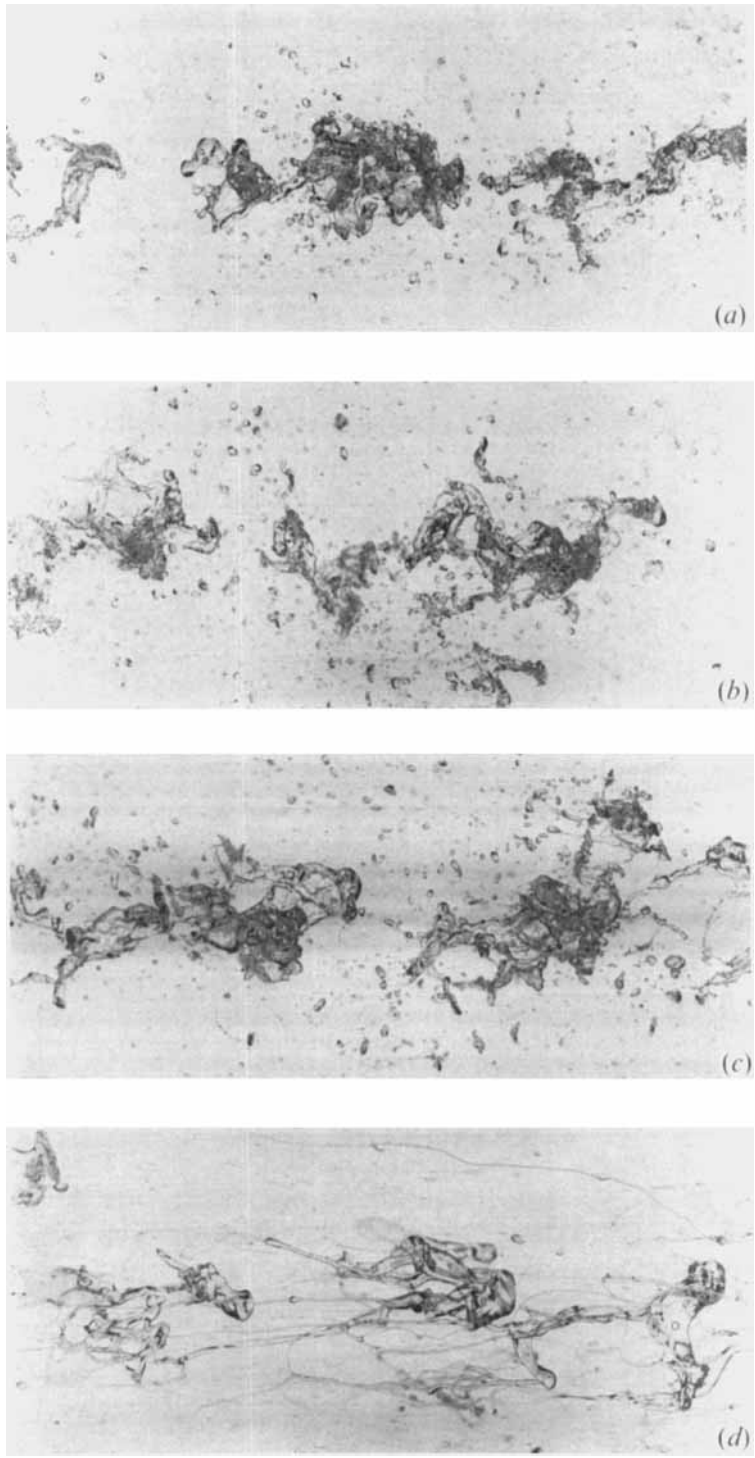

FIGURE 9. Appearance of jet from $\frac{1}{4}$ in. nozzle, 9 ft from nozzle exit. (*a*) Water. (*b*) 10 p.p.m. poly(ethylene oxide). (*c*) 50 p.p.m. (*d*) 200 p.p.m.

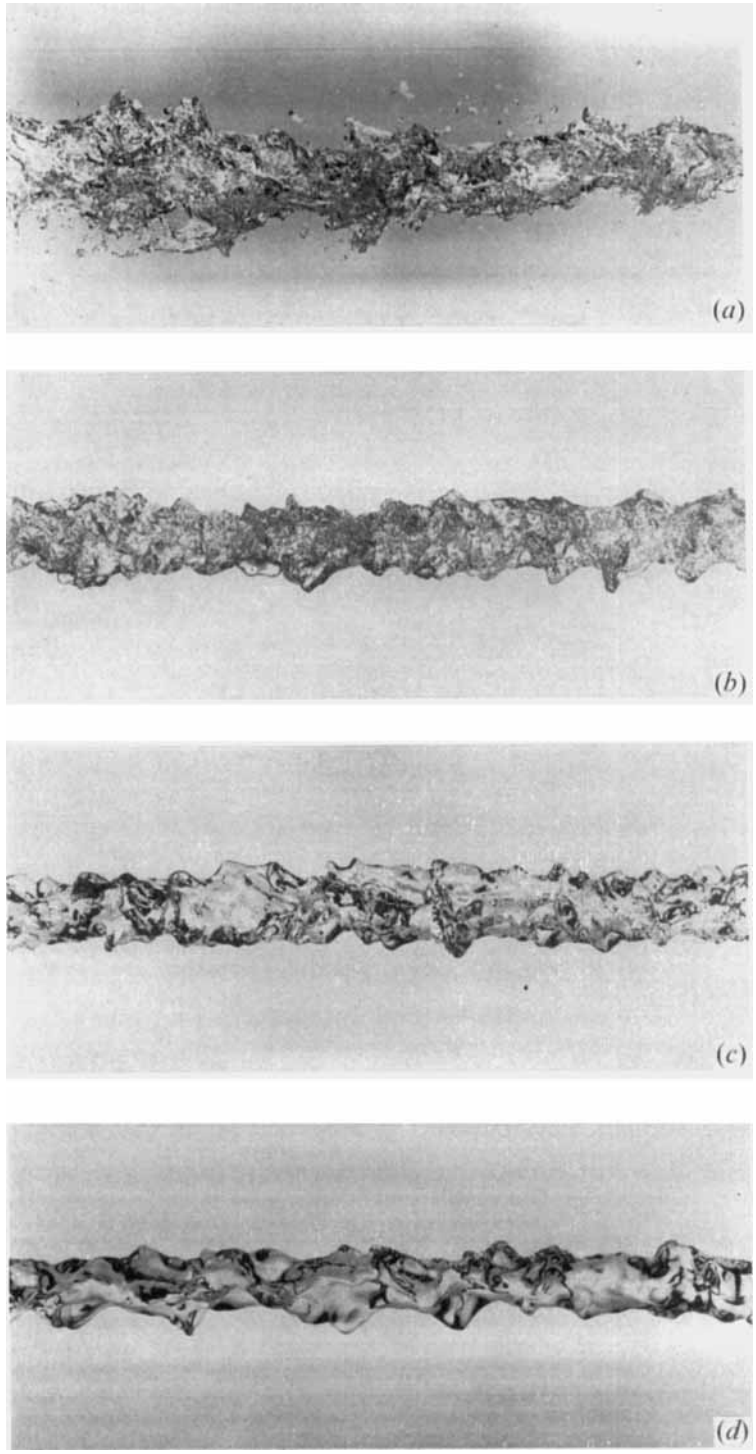

FIGURE 10. Appearance of jet from $\frac{1}{2}$ in. nozzle, 3 ft from nozzle exit. (*a*) Water. (*b*) 10 p.p.m. poly(ethylene oxide). (*c*) 50 p.p.m. (*d*) 200 p.p.m.

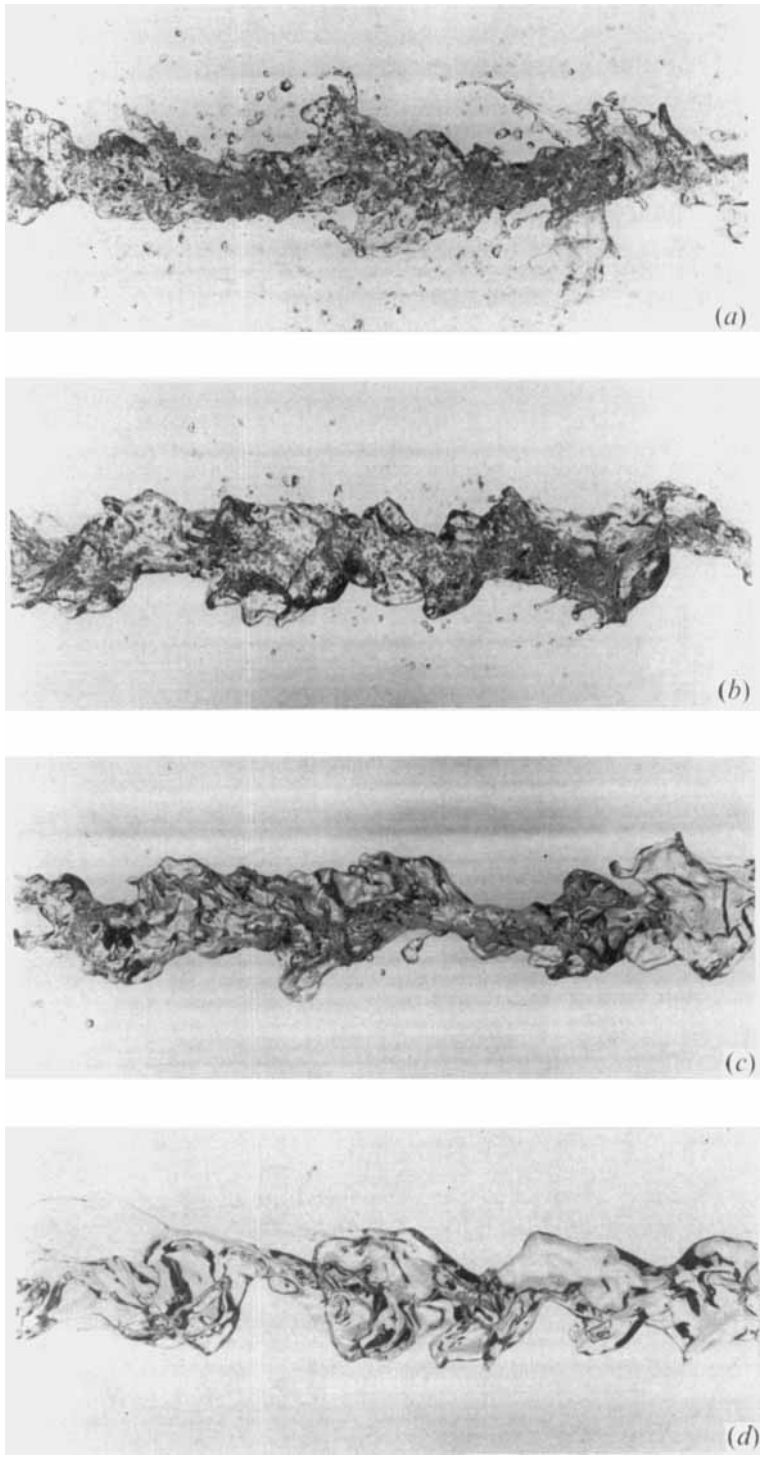

FIGURE 11. Appearance of jet from $\frac{1}{2}$ in. nozzle, 6 ft from nozzle exit. (*a*) Water. (*b*) 10 p.p.m. poly(ethylene oxide). (*c*) 50 p.p.m. (*d*) 200 p.p.m.

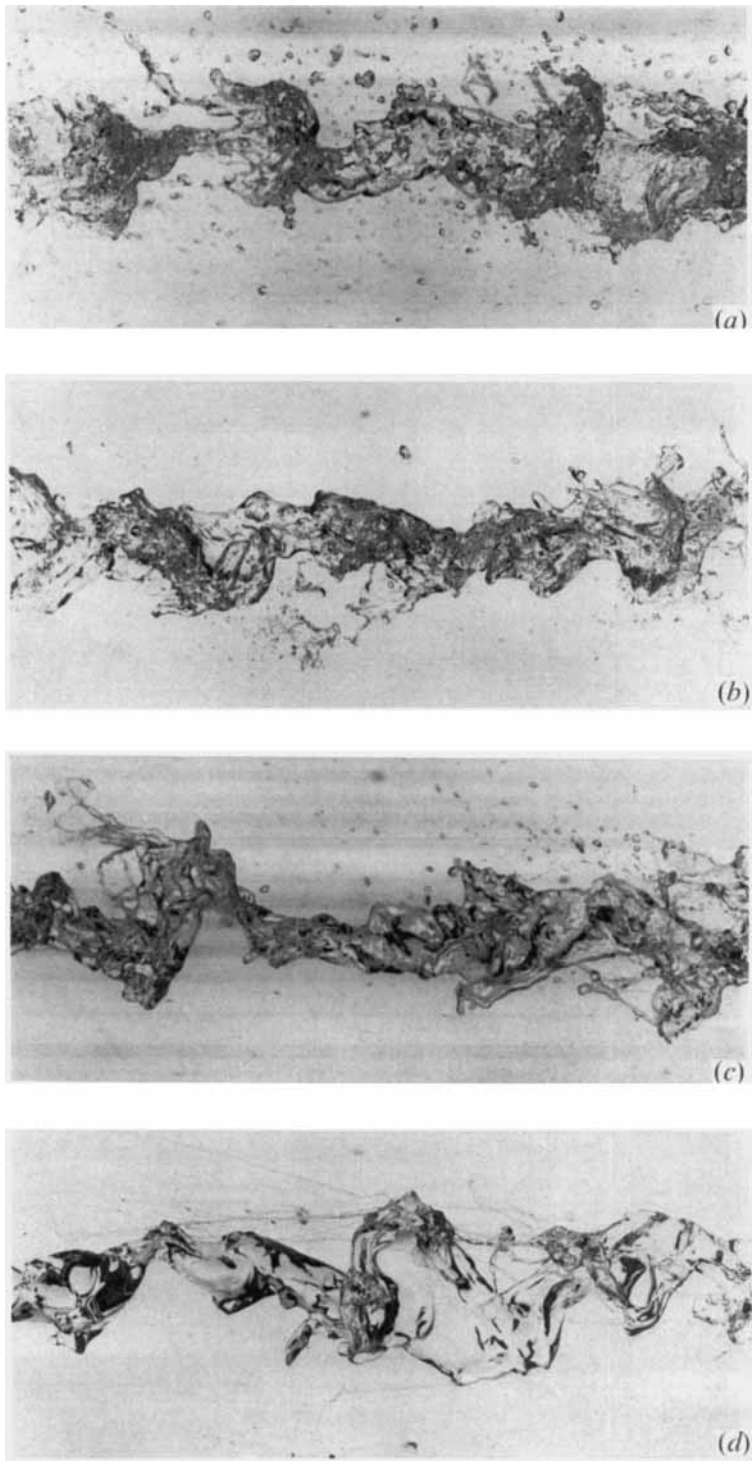

FIGURE 12. Appearance of jet from $\frac{1}{2}$ in. nozzle, 9 ft from nozzle exit. (*a*) Water. (*b*) 10 p.p.m. poly(ethylene oxide). (*c*) 50 p.p.m. (*d*) 200 p.p.m.

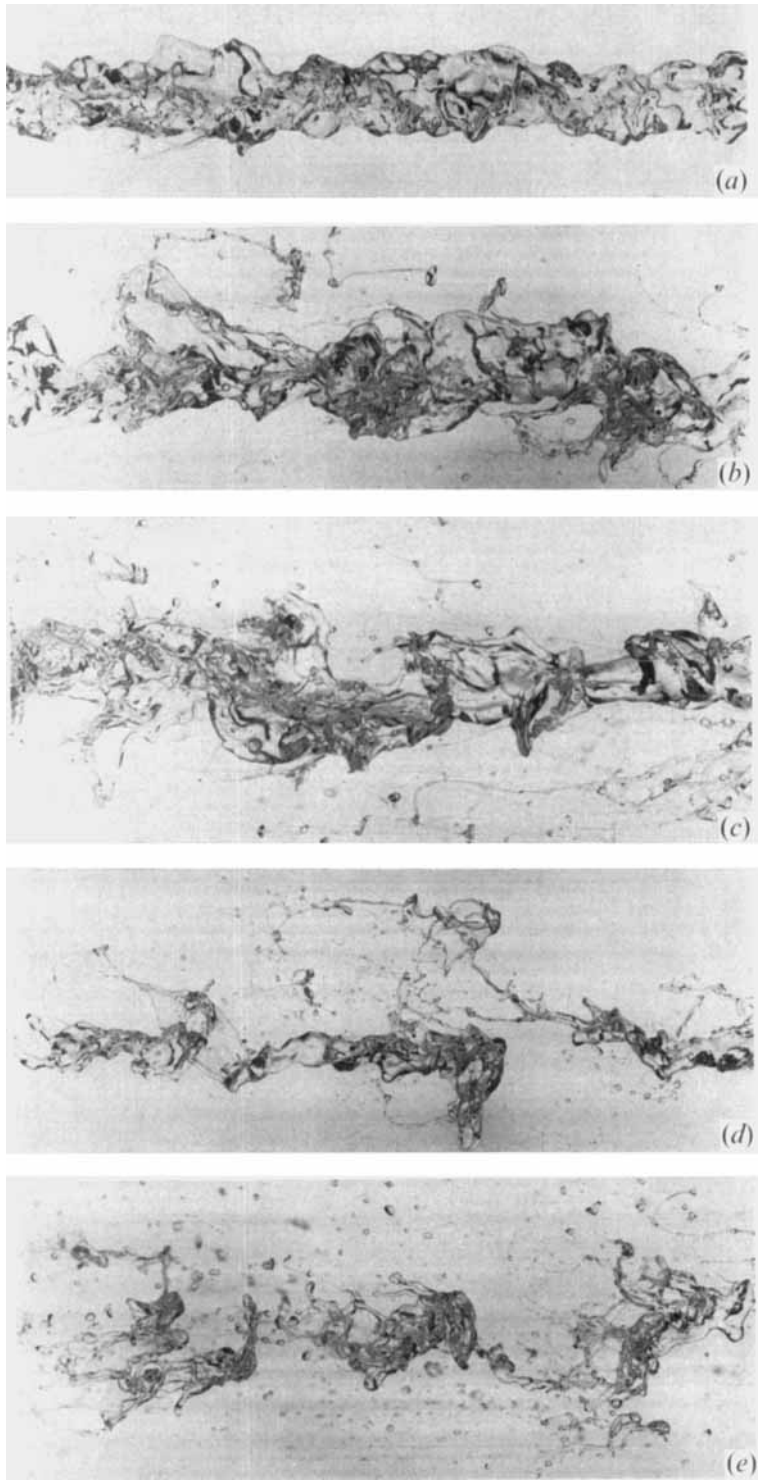

FIGURE 13. Appearance of jet of 100 p.p.m. poly(ethylene oxide) as a function of X/d. (*a*) $X/d = 72$. (*b*) $X/d = 144$. (*c*) $X/d = 216$. (*d*) $X/d = 288$. (*e*) $X/d = 432$.

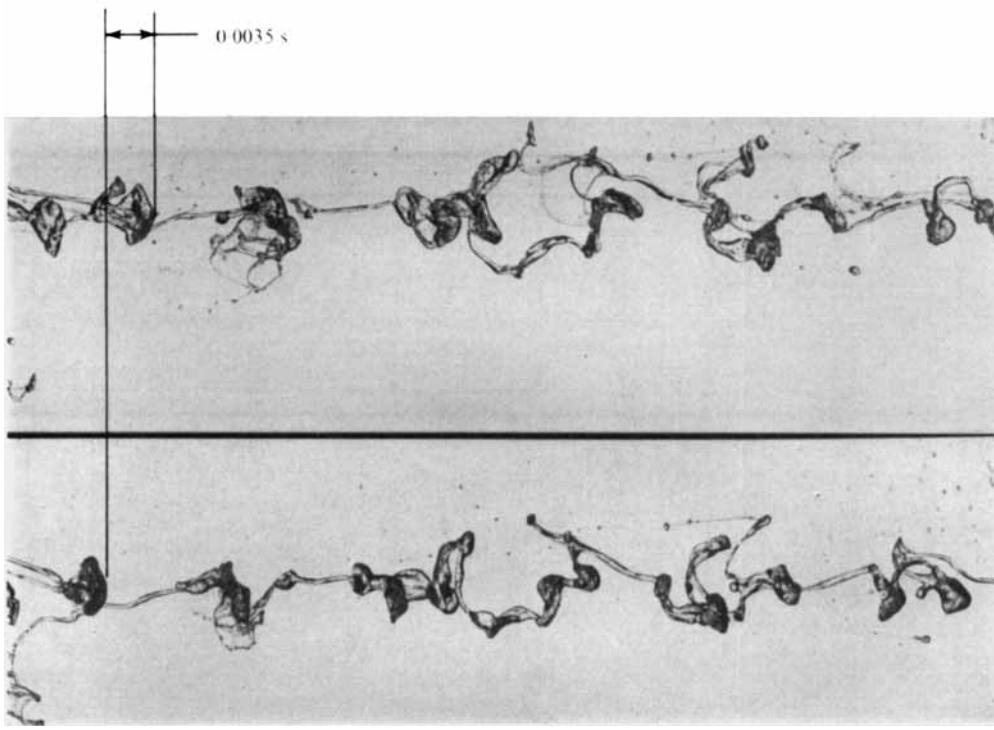

FIGURE 14. Appearance of 100 p.p.m. poly(ethylene oxide) jet from $\frac{1}{8}$ in. nozzle. Upper photo taken with 0·0035 s delay. (3 ft from nozzle exit.)

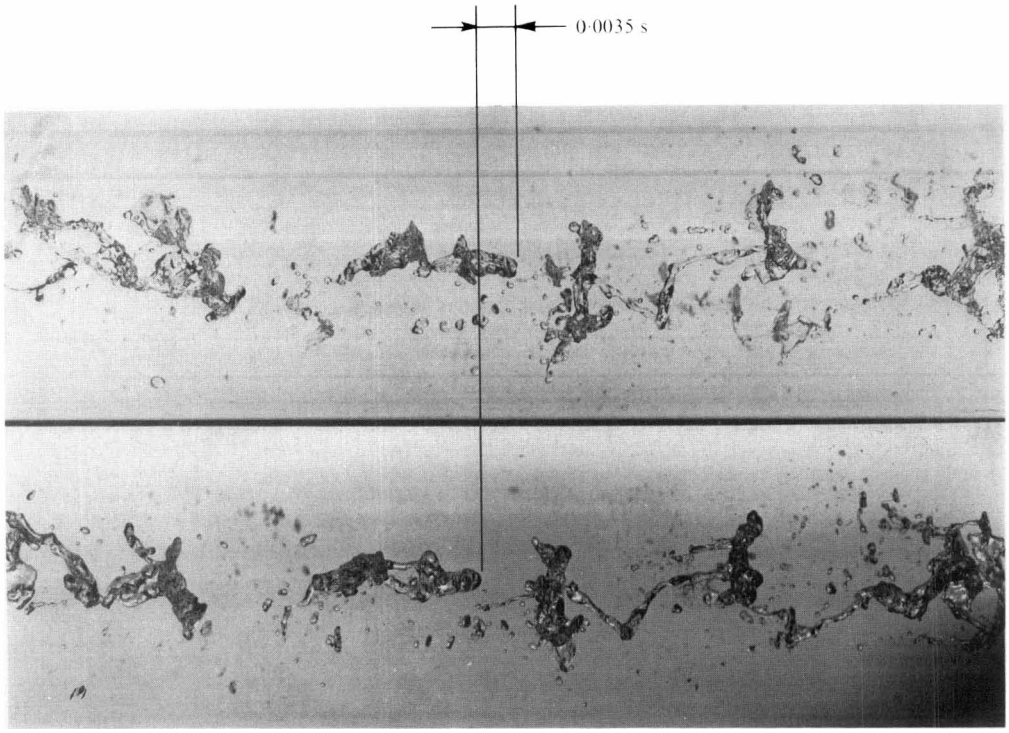

FIGURE 15. Appearance of water jet from $\frac{1}{8}$ in. nozzle. Upper photo taken with 0·0035 s delay. (3 ft from nozzle exit.)